

Understanding the limits to generalisability of experimental evolutionary models

Samantha E. Forde*¹, Robert E. Beardmore*², Ivana Gudelj*³, Sinan S. Arkin², John N. Thompson¹ & Laurence D. Hurst⁴

¹*Department of Ecology and Evolutionary Biology, University of California, Santa Cruz, CA 95064, USA*

²*Department of Mathematics, Imperial College London, London SW7 2AZ, UK*

³*Department of Mathematical Sciences, University of Bath, Bath BA2 7AY, UK*

⁴*Department of Biology & Biochemistry, University of Bath, Bath BA2 7AY, U.K.*

**co-first authors*

Given the difficulty of testing evolutionary and ecological theory *in situ*, *in vitro* model systems are attractive alternatives¹. But can we appraise whether an experimental result is particular to the *in vitro* model, and, if so, characterize the systems likely to behave differently and understand why? We examine these issues employing as a case history the relationship between phenotypic diversity and resource input in the T7-*Escherichia coli* co-evolving system. We establish a mathematical model of this interaction, framed as one instance of a super-class of host-parasite co-evolutionary models, and show that it captures experimental results. By tuning this model we then ask how diversity as a function of resource input could behave for alternative co-evolving partners (e.g. *E. coli* with *lambda* phage). In contrast to populations lacking phage, variation in diversity with differences in resources is always found for co-evolving populations, supporting the geographic mosaic theory of coevolution². The form of this variation is not, however, universal. Details of infectivity are pivotal: in T7-*E. coli* with a modified gene-for gene interaction, diversity is low at high resource input, whereas for matching-allele interactions, maximal diversity is found at high resource input. A combination of *in vitro* systems and appropriately configured mathematical models is an effective means to isolate results particular to the *in vitro* system, characterize systems likely to behave differently and to understand the biology underpinning those alternatives.

We start by considering a mathematical model tailored to the specific biology of the bacterium *Escherichia coli* and its bacteriophage T7/T3 (for brevity, we refer to T7, we might equally be modeling T3, Ref. ³) but framed in such a way that alternative co-evolving systems might also be analysed. The model tracks evolution in initially isogenic populations of co-occurring clonally reproducing bacteria (B_0) and phage (P_0) in the chemostat. Mutation occurs with a small but prescribed probability and the fitness of mutant bacteria and phage depend on every component of the system (formally, a genotype-by-genotype-by-environment interaction alias selection mosaic^{2,4}).

Although host and parasites, including bacteria and bacteriophage⁵, are often thought to interact along a continuum from gene-for-gene to matching alleles^{6,7} (see Fig 1a-b), neither of these models matches the known biology of the *E. coli*-T7 interaction as T7 phage have higher adsorption rates to wild-type *E. coli* than to contemporary hosts⁸⁻¹⁰. Thus, in our initial model, we suppose that the binding probabilities between bacteria and phage are graded (see Ref. ¹¹; Fig 1c).

The graded infection mechanism is understandable when the details of the biology are known. Relative resistance to these phage can be conferred through mutations that truncate lipopolysaccharides (LPS) found within the outer membrane, thus preventing adsorption of the phage^{10,12}. These truncations can be shallow or deep^{10,13}. Relative resistance is also conditioned by pleiotropic interactions between LPS and outer membrane proteins (OMPs) and is dependent on mutations in both (Supplementary information 6.3). For simplicity, we assume in wild-type bacteria (B_0) two character states at two loci, L and O. To capture the pleiotropy, we assume that mutations at these loci regulate the biosynthesis of LPS polymers such that the length of the LPS O-antigen

correlates with the phenotype $l = 4 - (2 \times L + O)$, yielding four phenotypes $B_0(L=0,O=0)$ with $l = 4$, $B_1(0,1)$ with $l = 3$, $B_2(1,0)$ with $l = 2$ and $B_3(1,1)$ with $l = 1$. We term the graded mechanism (Fig 1c) a *modified* gene-for-gene interaction due to its resemblance to gene-for-gene interactions (Fig 1a).

Assumptions about pleiotropy determine the form of the mutational matrix, M_b , between the four bacterial types. We have considered numerous matrices and find that results are strikingly insensitive (Supplementary information 6.3). Mutations in wild-type phage (P_0) occur on one locus with four possible alleles giving rise to one of three types denoted P_i (i from 1 to 3).

The core of the *E. coli* –T7 model is a 4 by 4 matrix, Φ , that defines the relative infectivities of each phage strain to each bacterial type:

$$\Phi = \begin{matrix} & P_0 & P_1 & P_2 & P_3 \\ \begin{matrix} P_0 \\ P_1 \\ P_2 \\ P_3 \end{matrix} & \begin{matrix} 1 \\ \lambda \\ 0 \\ 0 \end{matrix} & \begin{matrix} \lambda \\ \lambda v \\ 0 \\ 0 \end{matrix} & \begin{matrix} \lambda^2 \\ \lambda^2 v \\ \lambda^2 v^2 \\ 0 \end{matrix} & \begin{matrix} \lambda^3 \\ \lambda^3 v \\ \lambda^3 v^2 \\ \lambda^3 v^3 \end{matrix} & \begin{matrix} B_0 \\ B_1 \\ B_2 \\ B_3 \end{matrix} \end{matrix} \quad [1]$$

where $v < 2$ represents the change in adsorption rate due to the loss of a single sugar from bacterial LPS complex whereas $\lambda < 1$ is the corresponding change of adsorption rate due to alterations in the structure of phage tail-fibre protein (Supplementary Information 2.3.1)

We also incorporate two well-established trade-offs: increasing the range of resistance to phage leads to a decrease in growth rate¹⁴⁻¹⁶ and increase in the number of hosts a phage can infect comes at a reproductive cost through a combination of trade-offs with adsorption rate and burst size^{14,17}.

To predict bacterial densities we then write:

$$\begin{aligned}
\frac{dS}{dt} &= D(S_0 - S) - c\mu(S)\mathbf{B}^T, \\
\frac{d\mathbf{B}}{dt} &= \mathbf{M}_b(\mu(S) \cdot \mathbf{B}) - (\Phi\mathbf{P}) \cdot \mathbf{B} - D\mathbf{B}, \\
\frac{d\mathbf{P}}{dt} &= \mathbf{M}_p(\beta \cdot (\Phi^T \mathbf{B}) \cdot \mathbf{P}) - D\mathbf{P}
\end{aligned} \tag{2}$$

where \mathbf{B} denotes the vector of four bacterial densities while \mathbf{P} denotes the vector of four phage densities. The first equation of [2] describes the rate of change of resource concentration in the chemostat S with D the dilution rate and S_0 representing resource concentration in the input vessel. The consumption of resources is modeled through Michaelis-Menten bacterial growth function μ and resource conversion rate c while phage production is represented by a vector of burst sizes β (latent period was not explicitly modeled). The information regarding bacterial and phage mutations is embedded within 4x4 matrices \mathbf{M}_b and \mathbf{M}_p respectively while Φ^T represents the transpose of the adsorption matrix Φ (for further description of the model see Supplementary Information 2).

We fine-tune the model by employing experimentally observed mean rank ordering of bacterial types, obtained as follows. We coevolved populations of *E. coli* and phage in chemostats and then evaluated the phenotypic diversity of the phage-resistant hosts and phage density. We screened T7-resistant hosts as B_1 , B_2 and B_3 based on resistance or sensitivity to a series of reference bacteriophage (Table 1). From the experimental data we estimated ν to be 0.636 and λ to be 0.94, within the bounds of prior expectations.

The model predicts important differences between different environments (Fig 2c, Fig 3a). First, with resource input around 10 $\mu\text{g/ml}$ of glucose, the experimental results

should be more variable than under high resource input. Thus we predict that the same bacteria should be found at more similar frequencies in high resource replicates; this is seen (all data: Wilcoxon test $P=0.0015$; day 17 data: $P=0.03$). Similarly, the model correctly predicts a higher degree of variation between resource levels than within (Wilcoxon test $P=0.003$).

The model also predicts (Fig 3b) higher phage densities in the higher resource input experiment (Fig 4), which is observed (Wilcoxon test, $P=0.0003$; controlling for bacterial type, $P=0.02$). At low resource input, phage type P_2 is predicted to be in greatest abundance, followed by P_3 with other types present at much lower levels (Fig 4c). Given that both P_2 and P_3 have highest adsorption rate on B_1 , the model predicts type B_1 would have higher rates of infection than its competitors. This prediction qualitatively agrees with our experimental findings although, given the rarity of B_1 we could not establish significance (Fig 3b). By contrast, at high resource input the phage type P_3 is predicted to be most abundant (Fig 4c). As this type has higher adsorption rates on B_2 than B_3 , the model predicts that B_2 bacteria would be most infected, again in agreement with observation (Wilcoxon test, $P=0.008$; Fig 3b).

Given the concordance between theory and observation described above, we conclude that our deterministic mathematical model is fit for purpose. Next we consider the expected outcome were the matrix Φ specific to alternative host-parasite interactions anywhere along the continuum from gene-for-gene to matching alleles^{5,7,14,18-20}.

Importantly, in all instances of matching allele models, the system is predicted to behave differently from the modified gene-for-gene model presented here, with high diversity at high resource input (for discussion see Supplementary Information 6.1; a specific

example is shown in Fig 2b and Supplementary Fig 8). The interaction between lambda and *E. coli* is a form of lock and key mechanism¹⁸ with phage evolving progressively towards increased affinity for the host receptor¹⁹, hence this is an instance of a matching allele-like interaction (Fig 1b). Permitting weak infectivity to non-matching types does not alter the conclusion that diversity should be high at high resource input (see Supplementary Information 6.1). Certain gene-for-gene type matrices, a class considered common in many host-parasite interactions^{6,14}, can also give this result (Fig 2a). However there are other matrices that might be deemed gene-for-gene that give the alternative result (see Supplementary Information 6.2).

More generally, we can show that as resource input increases from low to high, we observe two classes of outcome: a monotonic form as predicted for matching allele-like interactions (e.g. with lambda phage) in which diversity of bacteria is highest under high resource input and the inverted U-shaped form exemplified by T7 in which diversity is maximal at intermediate resource input. The extent to which diversity is below the maximum is dependent on the precise form of Φ and β . All models predict that diversity of coevolving hosts and parasites should vary with differences in resource input (e.g. Fig 2a-c). This contrasts with evolution in the absence of phage where there is no change in bacterial diversity with resource input. As different environments likely provide different resource inputs, creating a selection mosaic, co-evolution of phage and bacteria could drive between-environment differences in diversity, as conceived by the geographic mosaic theory of coevolution². The passage to a position of stasis at high resource input and the low diversity seen in the T7 case are not particular to assumptions about the number of alleles. So long as the matrix Φ is square and invertible, the number of alleles

has no effect on the available spectrum of diversity properties resulting from the mathematical model (see Supplementary Information 3).

Why is diversity in our study maximal at intermediate resource input? For phage to persist after lysis they need to be able to re-infect bacteria. At very low nutrient levels ($S_0 < 1$) bacterial density is so low that re-infection is unlikely, so phage cannot persist. Consequently the fastest growing bacteria alone are found. As resource supply increases ($10 > S_0 > 1$) bacterial density increases, leading to a zone where intrinsic bacterial growth advantage favours B_0 and B_1 , while greater resistance to phage favours B_2 and B_3 . With phage not dominating the system, this balance potentially enables all four bacterial types to be maintained and for the outcome to be sensitive to S_0 . For $S_0 > 10$ bacterial growth and density are both high, but B_0 and B_1 are both killed by phage. With bacteria acting essentially as machines converting glucose to phage, these two relatively sensitive types can no longer persist. The resultant diversity is then a balance between differences in growth rate and differences in phage resistance of B_2 and B_3 . Increasing bacterial growth rates are kept in check by increasing death rates, so bacterial density changes little. By contrast, in some alternative models, such as matching alleles, we do not necessarily see the removal of B_0 and B_1 because the ancestral types are not sensitive, hence diversity remains high. Given the above explanation, it is perhaps not surprising in retrospect that what is found for T7- *E. coli* interactions need not be true for other biologically viable modes of host-parasite coevolution. These results show how appropriately framed mathematical models aligned with experimental analysis can obviate the need to presume typicality of one model within a class.

METHODS SUMMARY

The Models. The model is based on systems of ordinary differential equations that generate a dissipative dynamical system with a GxGxE structure². The model was parameterized with data on *E. coli* and T7 (Supplementary Information 5). Long-term diversity was computed using a standard Newton-continuation algorithm and applied to the model in steady-state form.

The Experiment. Thirty ml communities were inoculated with isogenic strains of *E. coli* and of T7 in chemostats. High resource (1000 μ g/ml of glucose) and low resource (10 μ g/ml glucose) communities were established. Samples of the phage populations and T7-resistant hosts were isolated after 150 bacterial generations of the experiment. T7-resistant colonies were isolated by taking 10 μ L from each community, plating it with 50 μ L of the ancestral strain of T7 on agar plates and incubating the combined sample at 37°C overnight. Each colony was streaked on an agar plate to remove any residual T7 present in the cells and then grown overnight in the same medium as used in the pertinent community. T7-resistant colonies were screened using a series of phage that target the lipopolysaccharide core (LPS) and specific outer membrane proteins (OMPs) (Table 1). The bacteriophage screen determined whether changes in the resistance cells had affected LPS and/or OMPs. We determined the abundance of phage on different bacterial types present in the communities by adding 30 μ L of chloroform to 1000 μ L of a sample taken from each community and vortexing the mixture to kill any bacteria that were present. One hundred μ L of each sample of the phage population were plated on a lawn of each bacterial isolate to determine the abundance of phage on each of the three host

phenotypes. Phage were plated on bacterial isolates from the same chemostat from which they originated. "Efficiency of plating" was our measure of phage abundance.

Full Methods and any associated references are available in the online version of the full paper at www.nature.com/nature

Received xxx; accepted xxx.

1. Jessup, C.M. *et al.* Big questions, small worlds: microbial model systems in ecology. *Trends Ecol. Evol.* **19**, 189-97 (2004).
2. Thompson, J. *The Geographic Mosaic of Coevolution*, (Chicago University Press, Chicago, 2005).
3. Kruger, D.H. & Schroeder, C. Bacteriophage T3 and bacteriophage T7 virus-host cell interactions. *Microbiol. Rev.* **45**, 9-51 (1981).
4. Wade, M.J. The co-evolutionary genetics of ecological communities. *Nature Rev. Genet.* **8**, 185-195 (2007).
5. Buckling, A. & Rainey, P.B. Antagonistic coevolution between a bacterium and a bacteriophage. *Proc. R. Soc. Lond., B* **269**, 931-936 (2002).
6. Agrawal, A. & Lively, C.M. Infection genetics: gene-for-gene versus matching-alleles models and all points in between. *Evol. Ecol. Res.* **4**, 79-90 (2002).
7. Morgan, A.D., Gandon, S. & Buckling, A. The effect of migration on local adaptation in a coevolving host-parasite system. *Nature* **437**, 253-256 (2005).
8. Chao, L., Levin, B.R. & Stewart, F.M. Complex community in a simple habitat - experimental-study with bacteria and phage. *Ecology* **58**, 369-378 (1977).
9. Forde, S.E., Thompson, J.N. & Bohannan, B.J.M. Adaptation varies through space and time in a coevolving host-parasitoid interaction. *Nature* **431**, 841-844 (2004).
10. Qimron, U., Marintcheva, B., Tabor, S. & Richardson, C.C. Genomewide screens for *Escherichia coli* genes affecting growth of T7 bacteriophage. *Proc. Natl. Acad. Sci. USA* **103**, 19039-19044 (2006).
11. Sasaki, A. & Godfray, H.C.J. A model for the coevolution of resistance and virulence in coupled host-parasitoid interactions. *Proc. R. Soc. Lond., B* **266**, 455-463 (1999).
12. Tamaki, S., Sato, T. & Matsuhara, M. Role of lipopolysaccharides in antibiotic resistance and bacteriophage adsorption of *Escherichia coli* K-12. *J. Bact.* **105**, 968-975 (1971).
13. Sen, K. & Nikaido, H. Lipopolysaccharide structure required for *in vitro* trimerization of *Escherichia coli* OmpF porin. *J. Bact.* **173**, 926-928 (1991).
14. Poullain, V., Gandon, S., Brockhurst, M.A., Buckling, A. & Hochberg, M.E. The evolution of specificity in evolving and coevolving antagonistic interactions between a bacteria and its phage. *Evolution* **62**, 1-11 (2008).

15. Bohannan, B.J.M., Kerr, B., Jessup, C.M., Hughes, J.B. & Sandvik, G. Trade-offs and coexistence in microbial microcosms. *Anton Leeuw. Int. J. G.* **81**, 107-115 (2002).
16. Yoshida, T., Hairston, N.G. & Ellner, S.P. Evolutionary trade-off between defence against grazing and competitive ability in a simple unicellular alga, *Chlorella vulgaris*. *Proc. R. Soc. Lond., B* **271**, 1947-1953 (2004).
17. Ferris, M.T., Joyce, P. & Burch, C.L. High frequency of mutations that expand the host range of an RNA virus. *Genetics* **176**, 1013-22 (2007).
18. Weitz, J.S., Hartman, H. & Levin, S.A. Coevolutionary arms races between bacteria and bacteriophage. *Proc. Natl. Acad. Sci. USA* **102**, 9535-9540 (2005).
19. Spanakis, E. & Horne, M.T. Co-adaptation of *Escherichia coli* and coliphage *lambda vir* in continuous culture. *J. Gen. Microbiol.* **133**, 353-60 (1987).
20. Lenski, R.E. & Levin, B.R. Constraints on the coevolution of bacteria and virulent phage - a model, some experiments, and predictions for natural communities. *Am. Nat.* **125**, 585-602 (1985).

Supplementary Information is linked to the online version of the paper at

www.nature.com/nature.

Acknowledgements Thanks to Angus Buckling, Scott Nuismer, Kate Rich, Jason Hoeksema and Christine Jessup for their comments on an earlier version of this manuscript. L.D.H. is a Royal Society Wolfson Research Merit Award Holder. I.G. is supported by a NERC Advanced Fellowship. S.S.A. is funded by an ORS award and a studentship for the Department of Mathematics at Imperial College London. S.E.F. and J.N.T. are supported by National Science Foundation.

Author Information Correspondence and requests for materials should be addressed to L.D.H. (l.d.hurst@bath.ac.uk)

Table 1| Bacterial phenotypic diversity: (a) bacteriophage screen used to determine where mutations likely occurred in the T7-resistant bacteria; (b) bacteriophage screen used to designate host phenotypes. S = sensitive, R = resistant.

a

Bacteriophage	Mutation
T4	LPS
T2	ompF or LPS
Tu1a	ompF

b

		Phage			
		T7 WT	T4	T2	Tu1a
Bacteria	B ₀ WT	S	S	S	S
	B ₁	R	S	S	R
	B ₂	R	R	S	S
	B ₃	R	R	R	R

Figure 1| Infection mechanisms between bacteria (B) and phage (P). The thickness of the lines represents infectivity levels: (a) gene-for-gene with intrinsic cost of virulence⁶; (b) matching alleles; (c) modified gene-for-gene where infectivity is always highest on the ancestral host.

Figure 2| Bacterial diversity at steady state as a function of resource input as provided by the mathematical model for different infection mechanisms: (a) a gene-for-gene model with costs of infection and virulence (infection matrix Φ motivated by Agrawal and Lively⁶ with parameter $k = 1/2$ and burst sizes $\beta_0 = 304$, $\beta_1 = 153$, $\beta_2 = 153$, $\beta_3 = 72$); (b) matching alleles⁶, as found in lambda-E. coli using four equal burst sizes of 304 and (c) modified gene-for-gene. All other parameter values are given in Supplementary Information, Table 1, bacterial densities are denoted B_i with i taking values from 0 to 3 and B_0 denoting wild type. We computed these curves taking S_0 from the minimal value required to support phage up to 1000 $\mu\text{g/ml}$.

Figure 3| Experimentally derived bacterial diversity and phage abundance as a function of resource input. (a) Diversity of bacterial phenotypes, and (b) the abundance of phage on each bacterial type (\pm S.E.) from day 17 of the experiment.

Figure 4| Phage diversity at steady state as a function of resource input for different infection mechanisms: (a) a gene-for-gene model with costs of infection and virulence (infection matrix Φ motivated by Agrawal and Lively⁶ with parameter $k = 1/2$ and burst sizes $\beta_0= 304, \beta_1=153, \beta_2=153, \beta_3=72$); (b) matching alleles⁶, as found in lambda-E. coli using four equal burst sizes of 304 and (c) modified gene-for-gene. Phage densities are denoted by P_i where i takes values from 0 to 3 and P_3 denotes the phage type that can infect all bacterial types. We computed these curves taking S_0 from the minimal value required to support phage up to 1000 $\mu\text{g/ml}$ (See Supplementary Information, Table 1 for parameter values.).

METHODS

The Models

The model is based on systems of ordinary differential equations that each generate a dissipative dynamical system with a GxGxE structure². The model was parameterized with data on *E. coli* and T7 (Supplementary Information 5) and we concluded that there exists a globally attractive state of equilibrium densities that can be approached in an oscillatory manner. Thus, one can summarise long-term diversity by plotting resource input S_0 versus the equilibrium densities of bacterial and phage types computed using a standard Newton-continuation algorithm implemented in MATLAB and applied to the model in steady-state form.

The Experiment

Thirty ml communities were inoculated with isogenic strains of *E. coli* and of T7 in chemostats. Two types of communities were established by manipulating the input of limiting nutrients for the bacteria: high resource (1000 $\mu\text{g/ml}$ of glucose; three communities) and low resource (10 $\mu\text{g/ml}$ glucose; two communities). Samples of the phage populations and T7-resistant hosts were isolated after the initial invasion of the resistant mutants and after the host and parasitoid coevolved for over 150 bacterial generations of the experiment (initial sample, high resource = 19, low resource = 11; final sample, high = 11, low = 12 bacterial colonies across all chemostats). Please see Ref²¹ for average population sizes.

Phenotypic diversity of resistant hosts

T7-resistant colonies were isolated by taking 10 μL from each community, plating it with 50 μL of the ancestral strain of T7 (titer of approximately 1×10^8) on agar plates and incubating the combined sample at 37°C overnight. Note that measuring the phenotypic diversity of the resistant hosts guarantees that selection has occurred, and thus any phage that can attack the hosts must be host-range mutants. Each colony was then streaked on an agar plate to remove any residual T7 present in the cells and grown overnight in the same type of liquid medium as used in the original experiment (i.e. either high or low resources). Freezer stocks of each culture were then stored in glycerol at -80°C for future use.

T7-resistant colonies were then screened using a series of phage that target the lipopolysaccharide core (LPS) and specific outer membrane proteins OMPs (Table 1). The presence of LPS is involved in maintenance of cell integrity and impermeability whereas OMPs are involved in uptake of nutrients into the cell and outer membrane stability. The subscripts of the four types (B_0 - B_3) refer to the number of LPS-targeting reference phages to which the bacterial type is resistant (see Table 1b) and also orders the types according to their growth kinetics with B_0 having the highest and B_3 the lowest growth rate (see Supplementary Information).

Each bacterial isolate was grown overnight in the appropriate medium (high or low resource) and then streaked across twenty μL of each reference phage that had been dried on an agar plate to assess resistance. In combination, these screens allowed us to

determine bacterial phenotypes in the high and low resource communities. The proportions of each phenotype at the start and end of the experiment were then averaged over time.

Abundance of phage on different bacterial phenotypes

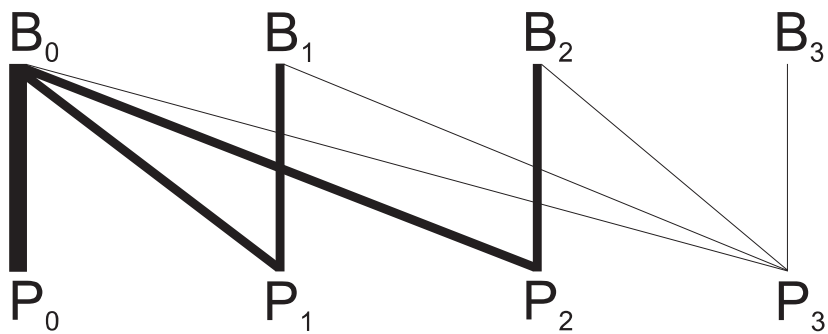
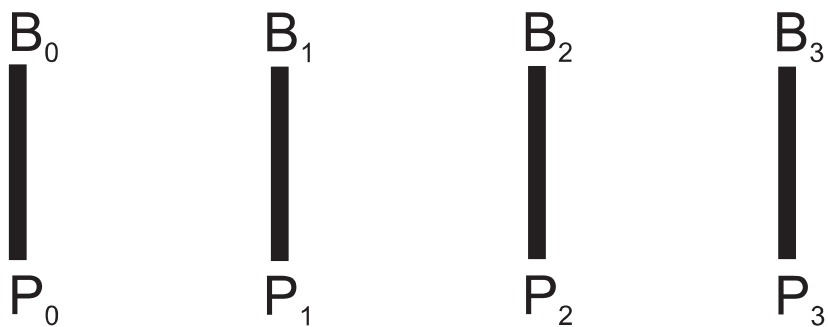
We determined the abundance of phage on different bacterial types present in the communities by adding 30 μ L of chloroform to 1000 μ L of a sample taken from each community and vortexing the mixture to kill any bacteria that were present. One hundred μ L of each sample of the phage population were plated on a lawn of each bacterial isolate to determine the abundance of phage on each of the three host phenotypes (B_1 , B_2 and B_3). Phage were also plated on ancestral bacteria (B_0). The number of phage plaques was consistently higher on B_0 . Phage were plated on bacterial isolates from the same chemostat from which they originated (5-7 isolates per chemostat) and we used the "efficiency of plating" (EOP; the number of plaques on each host) as a measure of phage abundance.

Data Analysis

We examined the prediction that there should be higher repeatability in experimental outcome at high resource input, for each of three bacterial types (B_1 , B_2 , B_3) by considering the modulus of the difference in the frequency of each type in each replicate experiment in a given resource level. In all replicates at high resource input there is no difference in the frequency of the each bacterial type. At low input the mean difference in frequency between replicate experiments is 0.21 +/- 0.08 (SEM) significantly greater than seen at high resource input (all data: Wilcoxon test $p=0.0015$; day 17 data: $P=0.03$).

We asked whether there is more variation between levels than within, by considering the modular difference in frequency of the same bacterial type between resource input levels and ask whether it is greater than the differences observed within resource levels, as predicted by the model: within resource level mean modular difference = 0.1 ± 0.03 (SEM) which is lower than the mean modular differences of frequencies observed at day 17 between the same bacterial types at difference resource levels (mean modular difference in bacterial frequency between resource levels = 0.37 ± 0.13 : Wilcoxon test $P=0.003$).

21. Forde, S.E., Thompson, J.N. & Bohannan, B.J. Gene flow reverses an adaptive cline in a coevolving host-parasitoid interaction. *Am Nat* **169**, 794-801 (2007).

a**b****c**